Recognizing relationship between groundwater level and hydrological time series (Case study: Ardabil plain)

Farnaz Daneshvar Vousoughi (fdaneshvar.vousoughi@gmail.com)
Islamic Azad University Ardabil Branch

Research Article

Keywords: Ardabil plain, groundwater level, wavelet transform coherence, wavelet-entropy measure, rainfall, runoff

Posted Date: December 28th, 2021

DOI: https://doi.org/10.21203/rs.3.rs-1182837/v1

Recognizing relationship between groundwater level and hydrological time series (Case study: Ardabil plain)

Farnaz Daneshvar Vousoughi[1*]

[1*]Department of Civil Engineering, Ardabil Branch, Islamic Azad University, Ardabil, Iran.

Corresponding Author: *E-mail:* fdaneshvar.vousoughi@gmail.com

Abstract

Two approaches to identify the relation between hydrological time series (rainfall and runoff) and groundwater level (GWL) were used in the Ardabil plain. In this way, Wavelet-entropy measure (WEM) and wavelet transform coherence (WTC) as two approaches of wavelet transform (WT) were used. WEM have been considered as a criterion for the degree of time series fluctuations and WTC present common time-frequency space. In WEM calculation, monthly rainfall, runoff and GWL time series were divided into three different time periods and decomposed to multiple frequent time series and then, the energies of wavelet were calculated for each sub-series. The result showed WEM reduction in rainfall, runoff and GWL. The reduction of WEM presents the natural fluctuations decrease of time series. The reduction of entropy for runoff, rainfall and GWL time series were about 1.58, 1.36 and 29% respectively, it is concluded that fluctuation reduction of hydrological time series has relatively not more effect on the oscillation patterns of GWL signal. In this regard, it could be concluded that the human activities such as water driving from wells can be played main role in the reduction of GWL in Ardabil plain. WTC findings showed that runoff had most coherence (0.9-1) among the hydrological variables with GWL time series in the frequency bands of 4-8 and 8-16 months.

Key Words: Ardabil plain, groundwater level, wavelet transform coherence, wavelet-entropy measure, rainfall, runoff

Statements and Declarations

Competing Interests:

- The authors have no relevant financial or non-financial interests to disclose.
- The authors have no competing interests to declare that are relevant to the content of this article.
- All authors certify that they have no affiliations with or involvement in any organization or entity with any financial interest or non-financial interest in the subject matter or materials discussed in this manuscript.
- The authors have no financial or proprietary interests in any material discussed in this article.

1. Introduction

Groundwater (GW) is a major source to meet urban, industrial, and particular agricultural water requirements, especially for tropical and sub-tropical semi-arid regions (Siebert et al. 2010). GW systems include some features such as complexity, nonlinearity, being multi-scale and random, all governed by natural and/or anthropogenic factors, it is important to detect such changes using a precise measure of fluctuations which are involved in the time series of the process (Nourani et al. 2015). Many researchers pointed to the effect of climate parameters on the decrease of groundwater level (GWL) time series (Zwolsman & van Bokhoven 2007; Waibel et al. 2013; Chinnasamy & Ganapathy 2018). The effect of human activities such as GW abstraction, recharge and reservoir construction on the GW level fluctuations (Xue et al. 2014; Singh et al. 2016; Yang et al. 2017; Amaranto et al. 2018; Deng et al. 2018).

Recently, different methods have been presented to calculate the time series complexity and signals in different fields of science and engineering. The WEM can be used to identify the effective factor in fluctuation change. Shannon (1948) presented the entropy concept to access additional information about time series. Many researches have been investigated about Shannon entropy concept in order for analyzing signals (Bercher & Vignat 2000; Shardt & Huang 2013; Chen & Li 2014; Castillo et al. 2015; Singh & Cui 2015; Varanis & Pederiva 2015).

The conjunction of entropy and wavelet concepts has been used to develop a new complexity measure of WE (Rosso et al. 2006). In addition to the aforementioned studies, it should be noted that in past decades several methods have been proposed to measure the complexity and consequently time series change detection and modeling. For example, Fathian et al. (2016) used Seasonal Auto Regressive Integrated Moving Average (SARIMA) in order to study Urmia Lake's water level change. This article aims to identify the changes in the statistical characteristics in terms of trend, stationarity, linearity/nonlinearity and change point detection analyses. Vaheddoost & Aksoy (2017) calculate entropy in each proposed station with respect to the long run mean precipitation of the basin. Although only a few studies have been conducted in the field of watershed engineering, discussing the complexity changes (Li and Zhang, 2008), biomedical studies, it has been deduced that deeper sleep or anesthesia, diseasing and aging in human are leading to decrease in complexity of the related physiologic signals, (Goldberger et al. 2002). It can be concluded that the WEM is a new and efficient index to determine the complexity of time series, especially hydrological time series. Komasi and Sharghi (2019) used WE as a criterion for the degree of time series fluctuations. Their result showed the WEM of aquifer water level reduction in Silakhor plain indicates the decrease in natural GWL time series fluctuations. The results showed that fluctuation decrease of discharge time series has relatively more effect on GWL oscillation patterns in comparison to the rainfall and temperature time series. Also, it could be concluded that the climate parameters are not facing significant changes; thus, human activities played main role for the declining GWL in Silakhor plain.

Hydrological time series are often non-stationary, in which different factors may influence the patterns such as climate change, human activities, etc. (Nourani et al. 2015). The presence of seasonality in hydrological processes will lead to accurate calculation of complexity and fluctuations using WTC measures. A useful mathematical tool such as WTC to measure the relationship between rainfall and runoff is an essential step in restoration projects for Ardabil plain. The main purpose of WT analysis as a function of time is decomposing a signal into sub-series at several frequencies of time (Danandeh Mehr et al. 2014). For instance, Grinsted et al. (2004) gained physical relationships among geophysical time series using WT analyses.

Holman et al. (2011) applied WT approach to distinguish time-space nonlinear relationships between North Atlantic Oscillation (NAO) atmosphere teleconnection and GWLs. They used continuous WT and XWT to distinguish the cross-wavelet power of time series. Tremblay et al. (2011) used correlation and wavelet analyses and wavelet coherence to gain effect linkages between four climatic indices (the North Atlantic Oscillation (NAO), the Arctic Oscillation (AO), the Pacific-North American pattern (PNA) and the El Niño Southern Oscillation represented by the Multivariate ENSO Index (MEI)), GWL time series, as well as precipitation and temperature time series are investigated in three Canadian regions. The three Canadian regions studied show drastically different patterns of variability evolution for the hydrogeological records. Yu and Lin (2015) applied the integration of XWT to examine the non-stationary time-frequency relation between precipitation and GWL variations. Their results showed nonlinear and non-stationary rainfall–recharge relationships of a GW system which can be frequency and spatially due to different frequencies. In a similar study, Henderson et al. (2009) applied XWT and CWT to identify tiny fluctuations in GW as a result of daily pumping at the submarine. Kuss and Gurdak (2014) use singular spectrum analysis (SSA), WTC, and lag correlation to quantify the effects of the El Niño Southern Oscillation (ENSO) (2–7 year cycle), North Atlantic Oscillation (NAO) (3–6 year cycle), Pacific Decadal Oscillation (PDO) (15–25 year cycle), and Atlantic Multidecadal Oscillation (AMO) (50–70 year cycle) on precipitation and GWLs of the United States. The results indicate that GWLs are partially controlled by interannual to multidecadal climate variability and are not solely a function of temporal patterns in pumping. ENSO and PDO have a greater control than NAO and AMO on variability in GWLs across the U.S., particularly in the western and central. Yu and Lin (2015) proposed an integration of XWT and empirical orthogonal function (EOF) analysis to analyze the space–time nonlinear relationships between the rainfall and GW changes. The EOF method revealed three major space–time patterns of the GWLs in results. The cross wavelet transform (XWT) further identified the lagged effects between rainfall and GW changes. Duvert et al. (2015) analyzed the hydrodynamic response of an agricultural watershed located in southeast Queensland, Australia, to low and high-frequency fluctuations in precipitation which occurred in duration 25 years. The results identified strong internal variations in the precipitation input affecting surface water flow more substantially than GWLs. Statistically, significant episodes of WTC were found at a 2–4-year band between Niño3.4 index and GWLs for the upstream piezometers, especially during the 1995–2000 period, which may be related to a strong La Niña event. Oh et al. (2017) developed the combined use of dynamic factor analysis (DFA) and wavelet analysis to identify complex latent factors controlling GWL fluctuations in a riverside alluvial aquifer influenced by barrage construction. They found that major driving forces controlling GWL time series data in a complex hydrological setting can be identified and quantitatively evaluated by the combined use of DFA and WT and applying WTC. Nourani et al. (2018) applied WTC to identify the impacts of hydro-climatological time series on fluctuations of water level in lakes (Urmia Lake and Van

Lake) in the Middle East. After investigation, the coherencies between runoff and water level demonstrated maximum values (0.9–1) in the two lakes. Drewnik et al. (2018) examined the variability of GWLs and GW temperature in raised bogs located in the Bieszczady Mts. in southern Poland. The WTC results show that most visible response of peat bogs to weather conditions was observed in summer and autumn. Neves et al. (2019) examined the links between major large-scale atmospheric circulation modes and inter-annual to decadal oscillations in GWLs using WTC in Portugal. The results show non-stationary relationships that are nonetheless consistent in distinct period bands. The relatively higher frequency (<5 year period) contributions of East Atlantic (EA) and Scandinavia (SCAND) are difficult to set apart but their joint impact accounts for approximately 20% and 40% of the total variance of GWLs in the south and north of the country, respectively. Zhang et al. (2019) used WTC for analyzing the response of GWL to semi-diurnal tide (SDT). The results show strong correlations at 0.5-, 1-, and 15-day time scales (resonance periodicities), which are then used as prediction periods for ANN models. The predicted results also confirm that SDT and precipitation have great influences on GWL with better prediction in the filled layer. Rezaei and Gurdak (2020) used singular spectrum analysis (SSA), WTC, and lag correlation calculations to analyze and quantify the impacts of the ENSO, NAO, PDO, and AMO on hydro-climate variables of precipitation, temperature, lake level, GW fluctuations, soil moisture, vegetation coverage, and insolation clearness index in the Lake Urmia watershed. A moderate coherence between PDO and the GWLs in most adjacent aquifers has occurred at the >8-year period from ~1980 to 2015. Malakar et al. (2021) investigated the long-term impact of local-precipitation, global-climate cycles, and human influence on multi-depth GWLs using lag correlation analysis, WTC, and regression-based dominance analysis. They observed intuitive responses, i.e., rapid response in shallow GW and relatively delayed responses to the global climate patterns with increasing depth.

In the present study, the effect of rainfall and runoff changes is investigated on the GWL of Ardabil plain aquifer using both the WEM and WTC criteria. The Hydrological time series are very complicated, using WT by decomposing time series into sub-signals can analyze time series and provided accurate short and long term information on different level of resolution (Rajaee et al. 2010; Komasi & Sharghi, 2019).

2. Methods and Materials

2.1. Wavelet transform (WT)

The most recent hydrological usage of WT was developed by Labat (2005) and Sang (2013). The time-scale WT of a continuous-time signal, *x(t)*, is defined as (Mallat, 1998):

$$T(a,b)=\frac{1}{\sqrt{a}}\int_{-\infty}^{+\infty} g^{*}\left(\frac{t-b}{a}\right)x(t).dt \tag{1}$$

Where *g(t)* represents mother wavelet and (*) corresponds to complex conjugate. Factor *a is* the dilation parameter, and *b* denotes the temporal translation of *g(t)* which provides the inspection of time series around *b*. Due to the compact support of its basic operation, providing a time-scale localization of process is the key property of WT. Searching for the similarities between the signal and wavelet function is the main application of WT. The time series of real hydrological problems are typically very continuous in a discreet format, the discreet type of WT (Mallat, 1998):

$$g_{m,n}(t)=\frac{1}{\sqrt{a_0^m}}g^{*}\left(\frac{t-nb_0a_0^m}{a_0^m}\right) \tag{2}$$

m and *n* are integers which control the wavelet dilation and translation, respectively; a_0 is a specified fined dilation step greater than 1; and the location parameter is presented by b_0. The most common choice for parameters are a_0 = 2 and b_0 = 1. This power-of-two logarithmic scaling of dilation and translation is known as the dyadic grid arrangement. The dyadic wavelet can be written in more compact notation as (Mallat, 1998):

$$g_{m,n}(t) = 2^{-m/2} g(2^{-m} t - n) \tag{3}$$

For a discrete time series, x_i, the dyadic WT becomes (Mallat, 1998):

$$T_{m,n} = 2^{-m/2} \sum_{i=0}^{N-1} g(2^{-m} i - n) x_i \tag{4}$$

The discrete wavelet coefficient for scale $a=2^m$ and location $b=2^m n$ is defined by $T_{m,n}$. A finite time series, $X_N = \{X_i\}_{i=1}^{N-1}$ in Eq.20 is considered where $N=2^M$. Regarding this concept, the boundaries of m and n are $(0, 2^M - m - 1)$ and$(1, M)$, respectively.

Mallat (1998) introduced the inverse form of discrete WT as:

$$x_i = \overline{T} + \sum_{m=1}^{M} \sum_{n=0}^{2^{M-m-1}} T_{m,n} 2^{-m/2} g(2^{-m} i - n) \tag{5}$$

The inverse form of discrete WT in a plain format is as follows (Mallat, 1998):

$$x_i = \overline{T}(t) + \sum_{m=1}^{M} W_m(t) \tag{6}$$

Where $\overline{T}(t)$ and $W_m(t)$ define the approximation and detailed sub-signals at levels $m = 1, 2, \ldots, M$.

$W_m(t)(m = 1, 2, \ldots, M)$, provide the detailed signals which is able to catch small features of interpretational value in the data and the residual component, $\overline{T}(t)$, denotes the historic information of data.

As a result of WT and to capture the temporal relationships among non-stationary time series, WTC was proposed to determine the localized correlation coefficients and their phase relationships among non-stationary signals in time–frequency spaces in which a detailed explanation of WTC can be found in Torrence and Compo (1998).

For two different time series, X_n and Y_n (n presents time scale), with different WTs of $W_n^X(s)$ and $W_n^Y(s)$, cross WT (XWT) is $W_n^{XY}(s) = W_n^X(s)\, W_n^{Y*}(s)$, where (*) presents the complex conjugate. The cross-wavelet power is defined as $|W_n^{XY}(s)|$. XWT identifies regions in time-frequency space where two-time series show high common power, and thus, significance (Nourani et al., 2018).

In particular, WT investigates whether regions with broad common power in time-frequency space have a clear phase relationship which are the predictive of causality between time series (Grinsted et al., 2004). In time-frequency space, WTC also presents regions where two-time series co-vary, but do not generally have high power. For this reason, when analyzing two-time series to determine both causality and local co-variance, the WTC is necessary. In terms of XWT, the WTC of two-time series is given as (Grinsted et al., 2004):

$$R_n^2(s) = \frac{\left|S(s^{-1}W_n^{XY}(s))\right|^2}{S\left(s^{-1}\left|S(W_n^X(s))\right|^2\right).S(s^{-1}\left|S(W_n^Y(s))\right|^2)} \tag{7}$$

Where *S* is a smoothing operator defined by wavelet type used, and the entire expression is similar to that of a traditional correlation coefficient localized in time–frequency space. Matlab code used in this study for WTC analysis is defined in detail by Grinsted et al. (2004).

2.2.Wavelet- entropy

In order to calculate WE, time series are decomposed in level M using WT, then Shannon WE and related energies in each level are obtained. Finally the multi-scale entropy is measured. The energy at each resolution level m = 1,2,3,..., M , will be the energy of the detail time series

$$\mathrm{E_m} = \|\mathrm{r_m}\|^2 = \sum_\mathrm{n} |\mathrm{C(m)_n}|^2 \tag{8}$$

And the total of energy as (Rosso et al. 2006)

$$\mathrm{E_{total}} = \sum_\mathrm{m} \sum_\mathrm{n} |\mathrm{C(m)_n}|^2 = \sum_\mathrm{m} \mathrm{E_m} \tag{9}$$

WE can be normalized (relative WE) as below (Rosso et al. 2006):

$$\rho_m = \frac{E_m}{E_{total}} \quad (10)$$

Shannon entropy as a criterion of the degree of uncertainty, tranquility and redundancy has been considered. The concept of entropy was used for measuring relative complexity in static signals. The time series with more entropy, random values and irregularity, they experience high complexity. SWS or the Shannon WE by Shannon entropy was calculated below (Rosso et al. 2001).

$$SWS = -\sum_m \rho_m \, . \, \ln[\rho_m] \quad (11)$$

Where ρ_m is defined in Eq. (10). Thus the SWS is a measure of the degree of order/disorder the signal, giving adequate information about the underlying dynamical process associated with the signal (Rosso et al. 2002).

2.3.Study zone and data collection

The study zone of this research placed in plain of Ardabil (38°03′– 38°27′N and 47°55′–48°20′E) which is located in north-western Iran, and covers an area of about 990 km^2, as shown in Fig. 1. Also, the mean areal annual rainfall in the Ardabil plain is about 304 mm. the wettest month is May and the driest months of the region is known as August. The average temperature in the Ardabil plain recorded about 9^o C, it is noticeable to mention that this plain is known as the coldest region in Iran. In the Ardabil plain the mean number of freezing days reported about 130 days in a year. The main rivers of this plain includes of Balikhli-Chay, Qara-Chay and Qara-Su which are naturaly non-perennial and recharge Ardabil plain aquifers. The Balikhli-Chay and Qara-Chay flow in the Qara-Su in the north part of Ardabil plain (see Fig. 1). In this study, the GWLs of 15 piezometric stations (P1, P2, P3... P15) located in the Ardabil plain from the period of 1993 to 2018 selected to perform the trend analysis. The GWL altitude in the study zone varies from 1308 m to 1529 m above the mean sea level. Figure 1 shows the locations of the GW monitoring stations in the study area. Table 1 presented the statistical characteristics of Ardabil plain. In this research, the monthly rainfall, runoff and GWL time series are used for 1993 to 2018 (300 months) (see Figure 2).

3. Results and Discussions

The GWL faces 11.43m decrease in the level of Ardabil plain piezometers in during 1993-2018 time period. It is possible to study occurred changes in runoff and rainfall time series using WEM and to examine climate change and human factors and their interactions in the complexity decrease of GWL. According to Fig. 2, the mean GWL was approximately 1341.45 m, max and min were 1346.75 m and 1335.40 m in 1993 and in 2018, it was about 11.43m decreased in 25 years' time period due to human activities and climate change effects in Ardabil plain. In this way, the mean GWL time series is separated to three subseries and WE measure is computed for each period. Sub series of GWL time series are consisted of 100 months of monthly data. The subseries of GWL by db2 mother wavelet decomposed to 5 subseries contain multiple frequent time series in level 1-5. The time series decomposition into different scales by WT introduce structure interpretation of series and determine knowledge about frequency domains and history of signal (Rajaee et al. 2010; Nourani et al. 2015). The db2 wavelet function is selected due to the similarity between db2 signal shape and the GWL time series fluctuations compared to other wavelet functions (Komasi & Sharghi, 2019). The WEM as complexity measure were applied to each three sub-series of GWL time series. Finally, the energy in normal form (ρ_n) was computed for decomposed sub-series of GW signal (levels 1 to 5). The results of normalized energy for decomposed GW signal are presented in Table 2. WEM in second time period (2001-02 to 2009-10), faces significant decrease which represents complexity decrease in GW signal of Ardabil plain. As presented in Table 2, WEM of GWL signal presents about 28.9922% reduction in the third part of time period (2009-10-2017-18). The decrease of WEM in a time period is presented unfavorable trend in GWL signal. Also, the WEM reduction indicates the decrease of complexity or the decrease of fluctuations in GWL signal at the third time period. As a result, the existence of undesirable trends in the GWL of Ardabil plain and the main aim is to assess the causes of GWL reduction through human activities and climate change factors.

The WEM of GWL decreased showing significant changes thus for finding dominant reason of GWL decrease in Ardabil plain, runoff and rainfall signals are examined. Also, in order to investigation the relations between rainfall (or runoff) and GWL parameters, WTC method is used.

To access this aim, runoff time series as human activities factors (Komasi & Sharghi, 2019) and rainfall time series of Ardabil plain as climate change factors (Komasi & Sharghi, 2019) are divided into three time sub-series with equal number (100-month). Then, the db4 mother wavelet decomposed each time sub-series to multi-frequent time series in decomposition levels 1 to 5 as GWL parameter. This part tries to identify human and climatic reasons that led to declining GWL. Similarly, divided sub-rainfall (or runoff) can be identified as the dominant reason for GWL reduction. Finally, WEM were estimated for three sub-series of rainfall and runoff signals. Tables 3–4 showed WEM for rainfall and runoff time series. Table 3 appears that the rainfall time series shows a WEM reduction of about -2.94016% and -1.360983% in the second and third time period. Hence, -2.94016% and -1.360983% reduction of fluctuations occurred in the second and third time period of the rainfall time series. Also, Table 4 indicates the WEM for the runoff time series present 0.86613% increase and -1.57813% decrease in the second and third time period respectively, it may not have a significant impact on the GW declining. Runoff vibration rate in 3 sub series shows increased value at second part and the decline of WEM value in third part. It is found that human activities led to runoff reduction of

Ardabil plain in third time period. In other words, runoff complexity is decreasing in third period. Dam constructions and irrigation as human activities result into runoff reduction, therefore complexity changes are decreased in third part. The WEM of rainfall and runoff time series in Tables 3 and 4 for can be compared with the WEM of GWL in Table 2 which shows both of rainfall and runoff signals play little role in the reduction of WEM for GWL signal in the third part of time period. The increase of WEM of GWL signal in the first time period could be effect from the increase of WEM of runoff signal.

Fig. 3 presented the WEM changes in 3 sub series for rainfall, runoff and GWL parameters in three 100-month periods. This Figure showed WE changes in the rainfall, runoff and GWL time series in best form. Also, this Fig. presented the WEM reduction of GWL, which indicates fluctuations or complexity decrease for the GWL signal of Ardabil plain, is much more than runoff and rainfall series in the third time period. It can be deduced that runoff complexity reduction is more than rainfall parameter reduction in the third part has effect on complexity decrease in GWL time series which none of them can be significant in the WEM reduction of GWL time series. Recently, human activities such as over-exploitation of GW has led to the GWL reduction in Ardabil plain, respectively. As a result, the GW exploitation plays important role in the decline of GWL in comparison to climate parameters such as rainfall time series.

To evaluate the coherency and also the seasonality relationship between hydrological time series (runoff and rainfall) and GWL time series, XWT and WTC were applied to time series of Ardabil plain. Coherence works like correlation, dark color indicates two-time series are strongly correlated within the bold black lines 1 (yellow), and the remaining 0 (blue) means no correlation or low correlation. Areas inside the bold black lines have indicated the times and periodicities with statistically significant XWT and WTC at the 5 percent significance stage. WTC calculates the cross correlation of two time series as a frequency function (at several wavelet scales).

XWT and WTC outcomes between GWL and rainfall signals of Ardabil plain are presented in Fig. 4 (a and b). Figs. 5 (a and b) show the XWT and WTC between runoff time series and GWL, respectively.

Before applying WT to the original rainfall, runoff and GWL time series, it is necessary to standardize them (mean=0 and variance=1). Regarding the coherence results given Figs. 4(a) and 5(a) showed the frequency of 8–16 months between rainfall and GWL time series, also, between runoff and GWL time series is common periodicities, which illustrates the most coherency in most time period. Figs. 4(b) and 5(b) presented the frequency of 8–16 months is low correlation between hydrological time series and GWL time series in XWT graphs.

Moreover, the results of wavelet coherence between runoff and GWL signals showed almost similar behavior between rainfall and GWL time series due to frequency band.

Among WTC graphs between rainfall and GWL signals and runoff and GWL signals, runoff parameter showed a high coherency value in 8–16 month periods. A high degree of coherence occurs in most month over a time scale of 12 months. Uniform rightwards with delay less correlation confirmed high coherence.

4. Conclusions and Suggestions

The decrease of GWL because of water resources management defect led to an important problem in human society and the environment. In this research, the multi-scale WEM and WT coherence method are used to identify the linkage between GWL decrease and rainfall or runoff time series in order to identify accurate effect of human activities and climate change on GWL time series in Ardabil plain.

In this study, runoff as a factor of human activities and rainfall as a factor of climate changes play role in hydrological processes. In this way, GWL, rainfall and runoff signals of Ardabil plain are separated to three 100-month sub-series with decomposition levels 1-5 in WEM calculation. The rainfall and runoff sub-series were divided to several frequent sub-series using the db4 mother wavelet and GWL sub-series were decomposed by the db2 mother wavelet. At last, for each sub-series of GWL, rainfall and runoff time series, WEM were calculated.

The results demonstrate that the WE measure of mean GWL signal presents the decrease in the third time period. In third time period, the WE measure for rainfall and runoff signals looks toward a decline but the major reason for the WE reduction in GWL signal is other human activity factors (since 2009-10–2017-18).

The results of WTC and XWT analysis for recognizing maximum common local multi-scale correlations, and phase relationships between rainfall (or runoff) and GWL time series in Ardabil plain showed that time scale of 12 months present high coherency.

To complete this study, some recommendations are proposed for future research; for instance, examining other hydro-climatological parameters effect in decreasing the GWL time series of Ardabil plain, such as human operations and climate variations in recent years. Furthermore, it is suggested to use the methodology of this research for other hydro-climatological parameters (e.g. temperature, transpiration …).

Compliance with Ethical Standards

The authors have no relevant financial or non-financial interests to disclose.

References

Amaranto A, Munoz-Arriola F, Corzo G, Solomatine D P, Meyer G (2018) Semi-seasonal groundwater forecast using multiple data-driven models in an irrigated cropland. J. Hydroinform 20 (6): 1227–1246.

Bercher J F, Vignat C (2000) Estimating the entropy of a signal with applications. IEEE Signal Process Soc 48 (6): 1687–1694.

Castillo A, Castelli F, Entekhabi D (2015) An entropy-based measure of hydrologic complexity and its applications. Water Resour Res 51 (7): 5145–5160.

Chen J, Li G (2014) Tsallis wavelet entropy and its application in power signal analysis. Entropy 16 (6): 3009–3025.

Chinnasamy P, Ganapathy R (2018) Long-term variations in water storage in Peninsular Malaysia. J Hydroinform 20 (5): 1180–1190.

Danandeh Mehr A, Kahya E, Bagheri F, Deliktas E (2014) Successive-station monthly streamflow prediction using neuro-wavelet technique. Earth Sci Inform 7: 217–229.

Deng X, Li F, Zhao Y, Li S (2018) Regulation of deep groundwater based on MODFLOW in the water intake area of the south-to-north water transfer project in Tianjin China. J Hydroinform 20 (4): 989–1007.

Drewnik M, Kuligiewicz A R, Stolarczyk M, Kucharzyk S, Żelazny M (2018) Intra-annual groundwater levels and water temperature patterns in raised bogs affected by human impact in mountain areas in Poland. Sci Total Environ 624: 991-1003.

Duvert C, Jourde H, Raiber M, Cox M E (2015) Correlation and spectral analyses to assess the response of a shallow aquifer to low and high frequency rainfall fluctuations. J Hydrol 527: 894-907.

Fathian F, Modarres R, Dehghan Z (2016) Urmia Lake waterlevel change detection and modeling. Model. Earth Syst Environ 2 (4), 203–219.

Goldberger A l, Peng C K, Lipsitz L A (2002) Fractal dynamics in physiology: alterations with disease and aging. Neurobiology of Aging 23: 23-26.

Grinsted A, Moore J C, Jevrejeva S (2004) Application of the cross wavelet transform and wavelet coherence to geophysical time series. Nonlin Process Geophys 11: 561–566.

Holman I P, Rivas-Casado M, Gurdak J J, Bloomfield J P (2011) Identifying non-stationary groundwater level response to North Atlantic Ocean-atmosphere teleconnection patterns using wavelet coherence. J Hydrol 19: 1269–1278.

Henderson R D, Day-Lewis F D, Harwey C F (2009) Investigation of aquifer-estuary interaction using wavelet analysis of fiber-optic temperature data. Geophys Res Lett 36: No.L06403.

Komasi M, Sharghi S (2019) Recognizing factors affecting decline in groundwater level using wavelet-entropy measure (case study: Silakhor plain aquifer). J Hydroinform 21(6): 510–522.

Kuss A J M, Gurdak J J (2014) Groundwater level response in U.S. principal aquifers to ENSO, NAO, PDO, and AMO. J Hydrol 519B: 1939-1952.

Labat D (2005) Recent advances in wavelet analyses: part 1—a review of concepts. J Hydrol 314: 275–288.

Li Z, Zhang Y K (2008) Multi-Scale entropy analysis of Mississippi River flow. Stoch Environ Res Risk Assess 22: 507-512 .

Malakar P, Mukherjee A, Bhanja S N, Ganguly A R, Ray R K, Zahid A, Sarkar S, Saha D, Chattopadhyay S (2021) Three decades of depth-dependent groundwater response to climate variability and human regime in the transboundary Indus-Ganges-Brahmaputra-Meghna mega river basin aquifers. Adv Water Resour 149: 103856.

Mallat S G (1998) A Wavelet Tour of Signal Processing, second ed. Academic Press, San Diego.

Nourani V, Komasi M, Alami M (2012) Hybrid wavelet– genetic programming approach to optimize artificial neural network k modeling of rainfall–runoff process. J Hydrol Eng 17 (6): 724–741.

Neves M C, Jerez S, Trigo R M (2019) The response of piezometric levels in Portugal to NAO, EA, and SCAND climate patterns. J Hydrol 568: 1105-1117.

Nourani V, Alami M T, Daneshvar Vousoughi F (2015) Wavelet-entropy data pre-processing approach for ANN-based groundwater level modeling. J Hydrol 524: 255-269.

Nourani V, Ghasemzade M, Danande Mehr A, Sharghi E (2018) Investigating the effect of hydroclimatological variables on Urmia Lake water level using wavelet coherence measure. J Water Clim Change DOI: 10.2166/wcc.2018.261 .

Oh Y Y, Yun S T, Yu S, Hamm S Y (2017) The combined use of dynamic factor analysis and wavelet analysis to evaluate latent factors controlling complex groundwater level fluctuations in a riverside alluvial aquifer. J Hydrol 555: 938-955.

Rajaee T, Mirbagheri S A, Nourani V, Alikhani, A (2010) Prediction of daily suspended sediment load using wavelet and neuro-fuzzy combined model. J Environ Sci Technol 7(1): 93–110.

Rezaei A, Gurdak J J (2020) Large-scale climate variability controls on climate, vegetation coverage, lake and groundwater storage in the Lake Urmia watershed using SSA and wavelet analysis. Sci Total Environ 724: 138273.

Rosso O A, Martin M T, Figliola A, Keller K, Plastino A (2006) EEG analysis using wavelet-based information tools. Neuroscience Methods 153: 163-182.

Rosso O A, Blanco S, Yordanova J, Kolev V, Figliola A, Schurmann M (2001) Wavelet entropy: a new tool for the analysis of short duration brain electrical signals. J Neurosci Methods 105: 65-75.

Rosso O A, Mairal M L (2002) Characterization of time dynamical evolution of electroencephalographic records. Physica A 312: 469-504.

Sang Y F (2013) A review on the applications of wavelet transform in hydrology time series analysis. Atmos Res 122: 8–15 .

Shannon C E (1948) A mathematical theory of communications I and II. bell Syst Tech J 27 (3): 379–443.

Shardt Yuri A W, Huang B (2013) Statistical properties of signal entropy for use in detecting changes in time series data. J Chemometr 27 (11): 394–405.

Siebert S, Burke J, Faures JM, Frenken K, Hoogeveen J, Döll P, Portmann FT (2010) Groundwater use for irrigation—a global inventory. Hydrol Earth Syst Sci 14: 1863–1880.

Singh M K, Singh, V P, Das P (2016) Mathematical modeling for solute transport in aquifer. J Hydroinform 18(3): 481–499.

Singh V P, Cui H (2015) Entropy theory for groundwater modeling. J Groundwater Res 3(4): 1–12.

Tremblay L, Larocque M, Anctil F, Rivard C (2011) Teleconnections and interannual variability in Canadian groundwater levels. J Hydrol 410(3-4): 178-188.

Vaheddoost B, Aksoy H (2017) Structural characteristics of annual precipitation in Lake Urmia basin. Theor Appl Climatol 128 (3–4): 919–932.

Varanis M, Pederiva R (2015) Wavelet packet energy-entropy feature extraction and principal component analysis for signal classification. Proc Brazil Soc Appl Comput Math 3(1): 1–7.

Waibel M S, Gannett M W, Chang H, Hulbe C L (2013) Spatial variability of the response to climate change in regional groundwater systems – examples from simulations in the Deschutes basin, Oregon. J Hydrol 486: 187–201.

Xue L, Guomin L, Yuan Z (2014) Identifying major factors affecting groundwater change in the north China plain with grey relational analysis. Water 6(6): 1581–1600 .

Yang Q, Zhang J, Hou Z, Lei X, Tai W, Chen W, Chen, T (2017) Shallow groundwater quality assessment: use of the improved Nemerow pollution index, wavelet transform and neural networks. J Hydroinform 19(5): 784–794.

Yu L H, Lin, C Y (2015) Analysis of space–time non-stationary patterns of rainfall–groundwater interactions by integrating empirical orthogonal function and cross wavelet transform methods. J Hydrol 525: 585–597.

Zhang J, Zhang X, Niu J, Hu B X, Soltanian M R, Qiu H, Yang L (2019) Prediction of groundwater level in seashore reclaimed land using wavelet and artificial neural network-based hybrid model. J Hydrol 577: 123948.

Zwolsman J J G, van Bokhoven A J (2007) Impact of summer droughts on water quality of the Rhine River – a preview of climate change. Water Sci Technol 56 (4): 45–55.

Figures Captions

Fig. 1. Case study and the position of piezometers.

Fig. 2. a) GWL b) Rainfall and c) Runoff time series of Ardabil plain.

Fig. 3. The WEM of rainfall, runoff and GWL time series in three periods

Fig. 4. a) WTC and b) XWT between runoff and GWL time series

Fig. 5. a) WTC and b) XWT between rainfall and GWL time series

Table 1. Statistical characteristics of Ardabil plain

Type of Time series	Max	Min	Mean	Variance
Groundwater Level (m)	1346.75	1335.40	1341.45	10.68
Rainfall (mm)	91.1	0	19.64	322.78
Runoff (m^3/s)	658.72	0	64.01	8914.47

Table 2. The Wavelet-entropy measure of groundwater level time series

Normal Energy For Groundwater level sub-series	**100 month sub-series**		
	Period 1	Period 2	Period 3
$\boldsymbol{\rho 1}$	0.160697	0.2771	0.137869
$\boldsymbol{\rho 2}$	0.333701	0.334202	0.210267
$\boldsymbol{\rho 3}$	0.356498	0.353261	0.235014
$\boldsymbol{\rho 4}$	0.216533	0.189869	0.224481
$\boldsymbol{\rho 5}$	0.30142	0.360019	0.267748
SWS	1.36885	1.514451	1.075378
		10.6367%	-28.9922%

Table 3. The Wavelet-entropy measure of rainfall time series

Normal Energy For Rainfall sub-series	**100 month sub-series**		
	Period 1	Period 2	Period 3
$\rho 1$	0.359293	0.363394	0.367306
$\rho 2$	0.367136	0.362254	0.364752
$\rho 3$	0.36007	0.316959	0.341205
$\rho 4$	0.106272	0.16316	0.122426
$\rho 5$	0.126035	0.074264	0.066921
SWS	1.318806	1.280031	1.26261
		-2.94016%	-1.360983%.

Table 4. The Wavelet-entropy measure of runoff time series

Normal Energy For Runoff sub-series	**100 month sub-series**		
	Period 1	Period 2	Period 3
$\boldsymbol{\rho 1}$	0.307985	0.335789	0.348264
$\boldsymbol{\rho 2}$	0.334151	0.312815	0.367716
$\boldsymbol{\rho 3}$	0.357349	0.355811	0.364868
$\boldsymbol{\rho 4}$	0.262108	0.223004	0.125844
$\boldsymbol{\rho 5}$	0.054845	0.100421	0.100194
SWS	1.316438	1.32784	1.306885
		0.86613%	-1.57813%

Figures

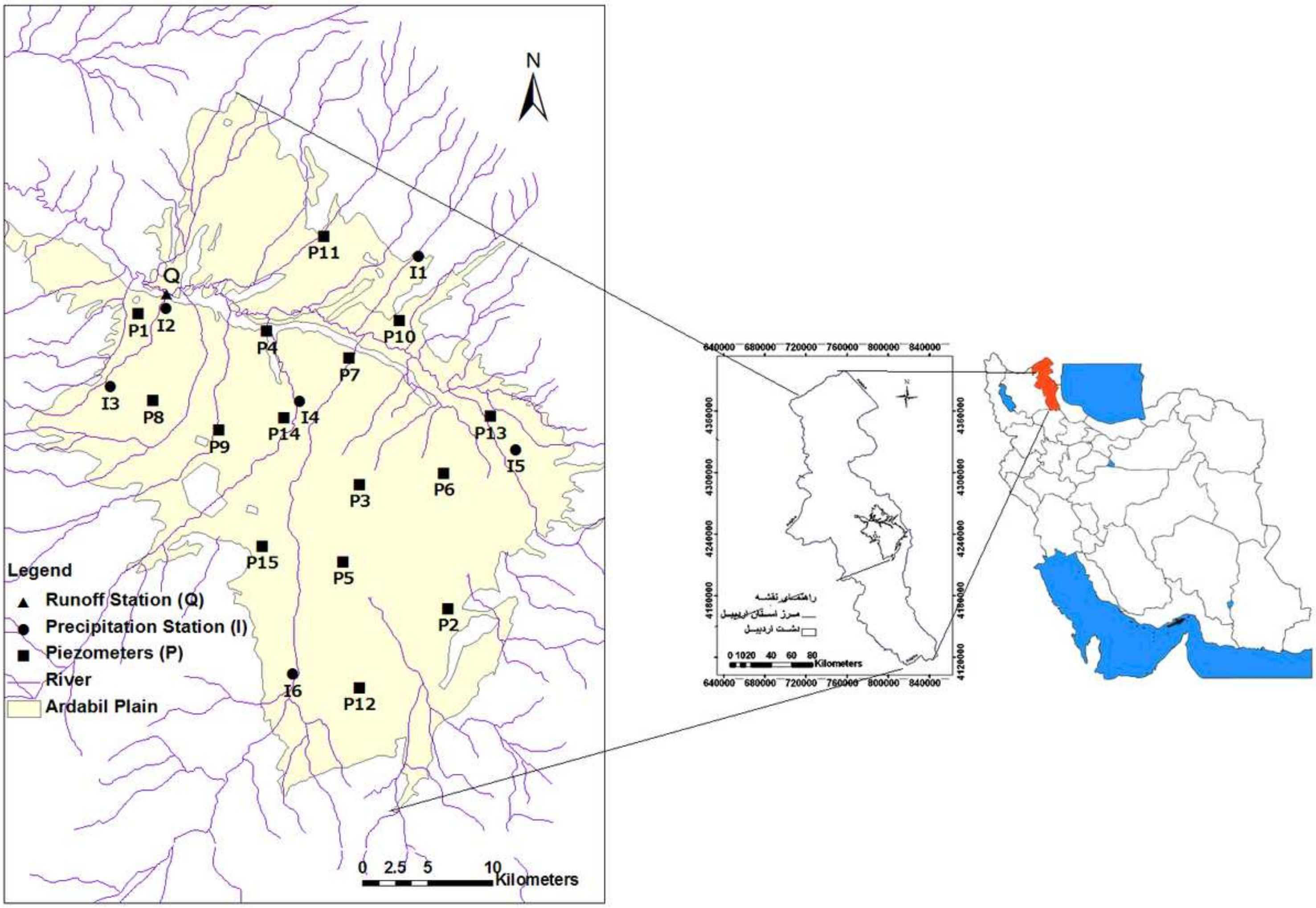

Figure 1

Case study and the position of piezometers.

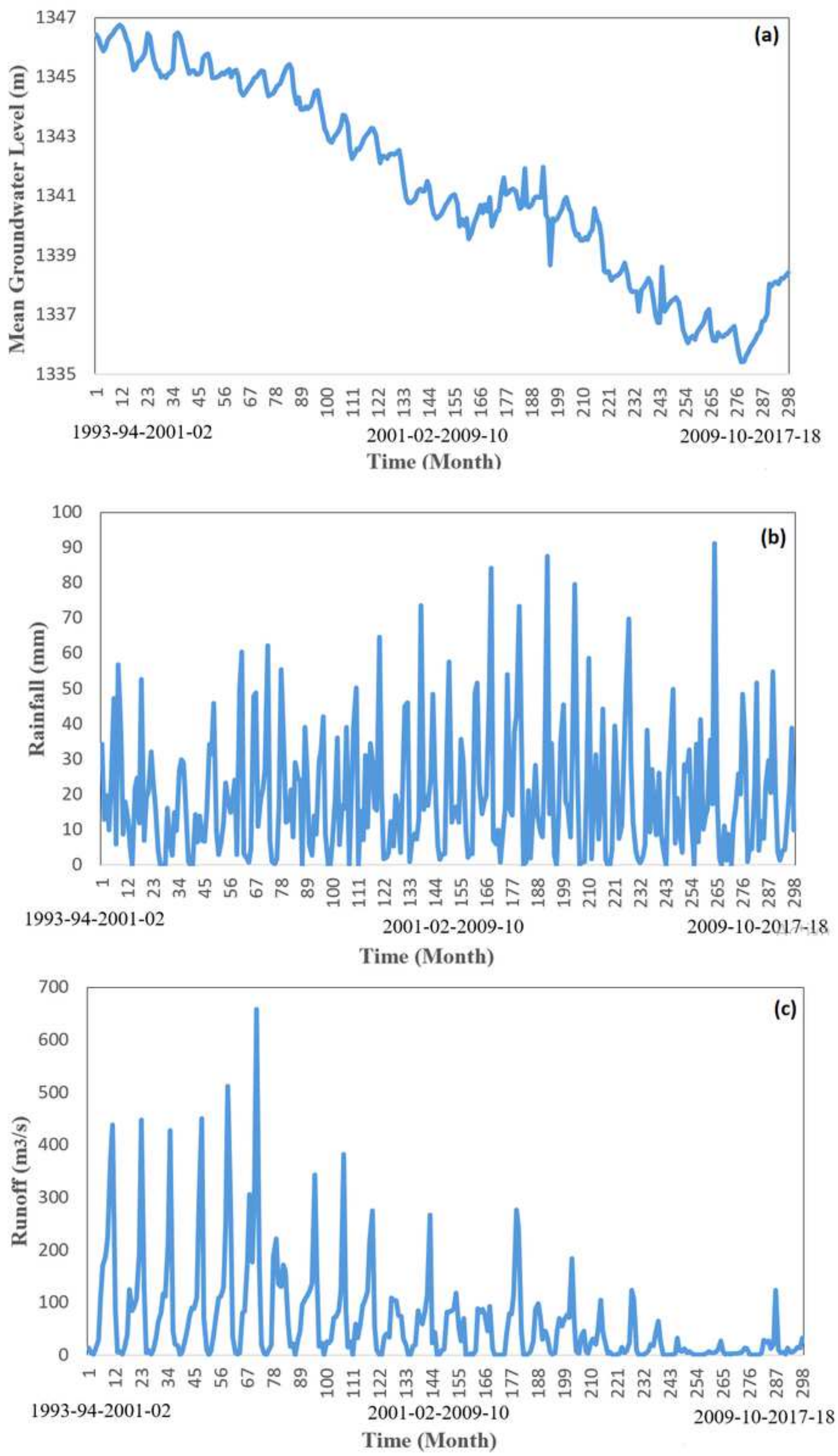

Figure 2

a) GWL b) Rainfall and c) Runoff time series of Ardabil plain.

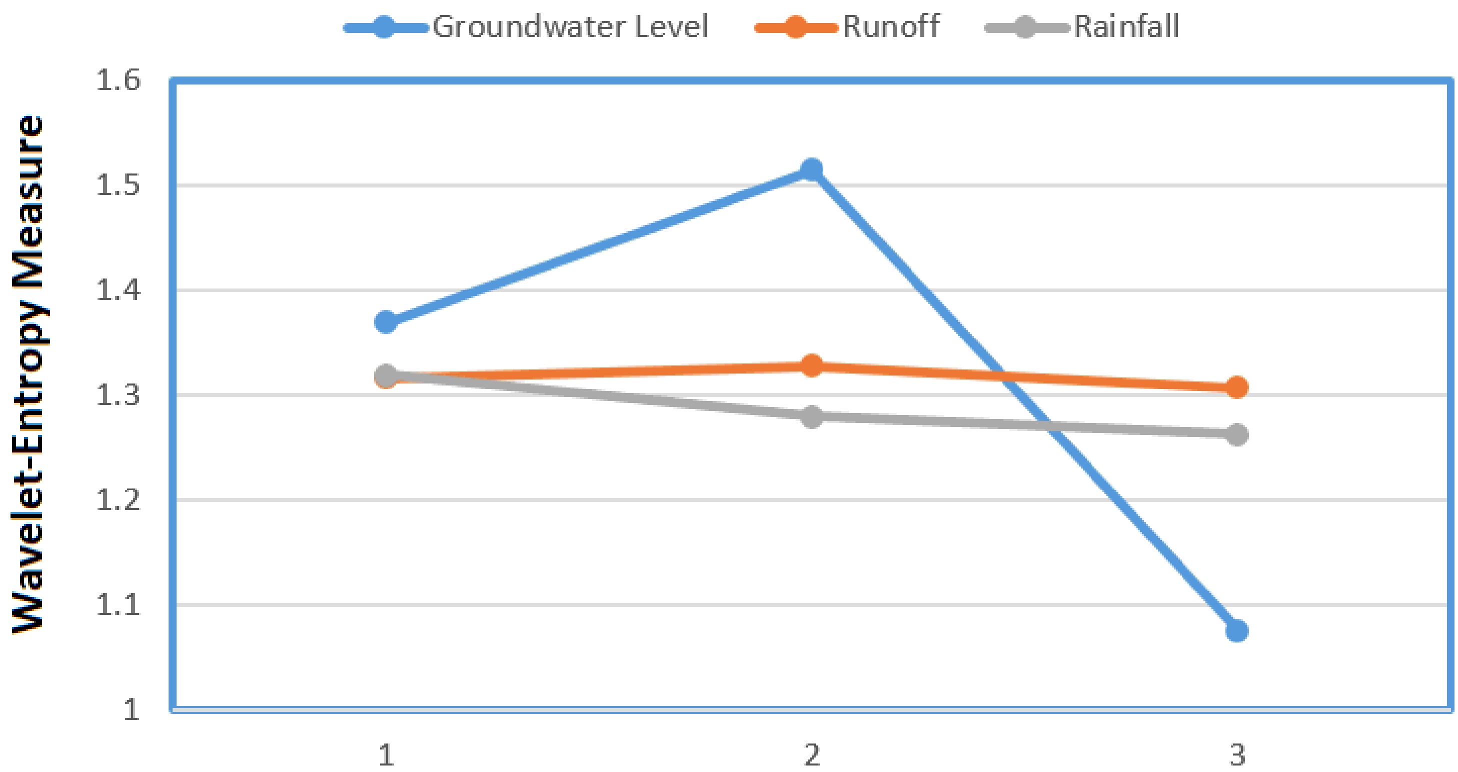

Figure 3

The WEM of rainfall, runoff and GWL time series in three periods

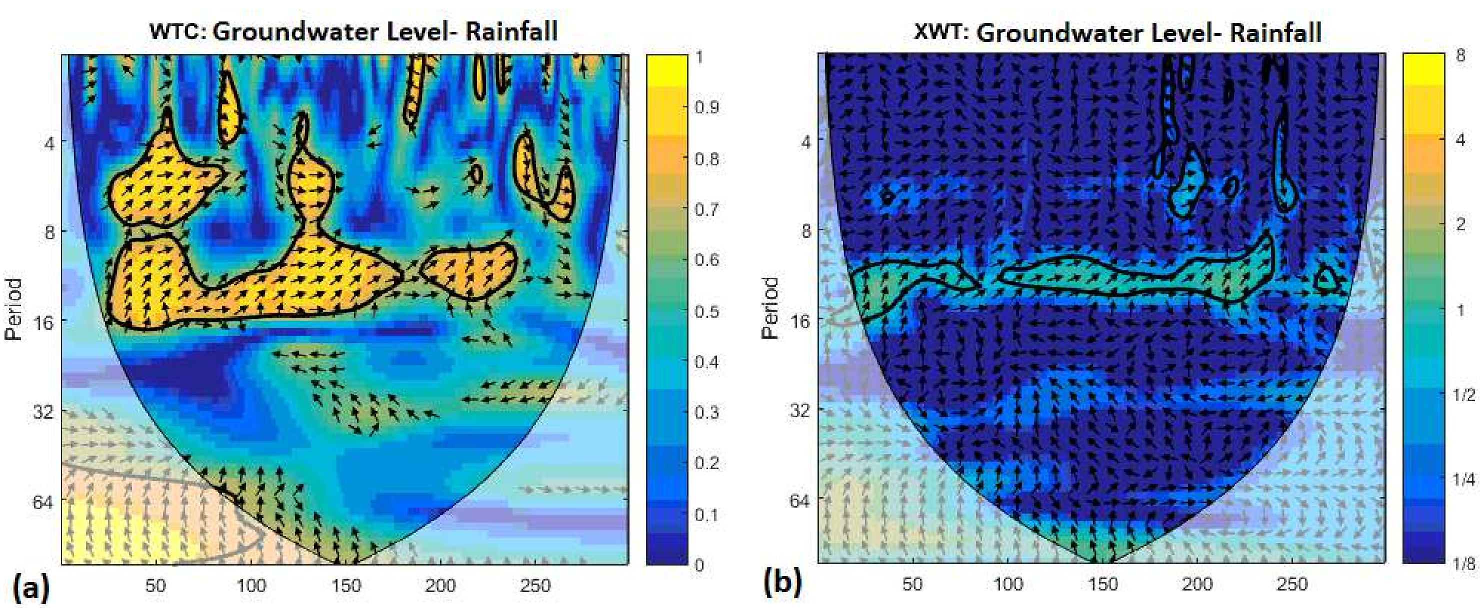

Figure 4

a) WTC and b) XWT between runoff and GWL time series

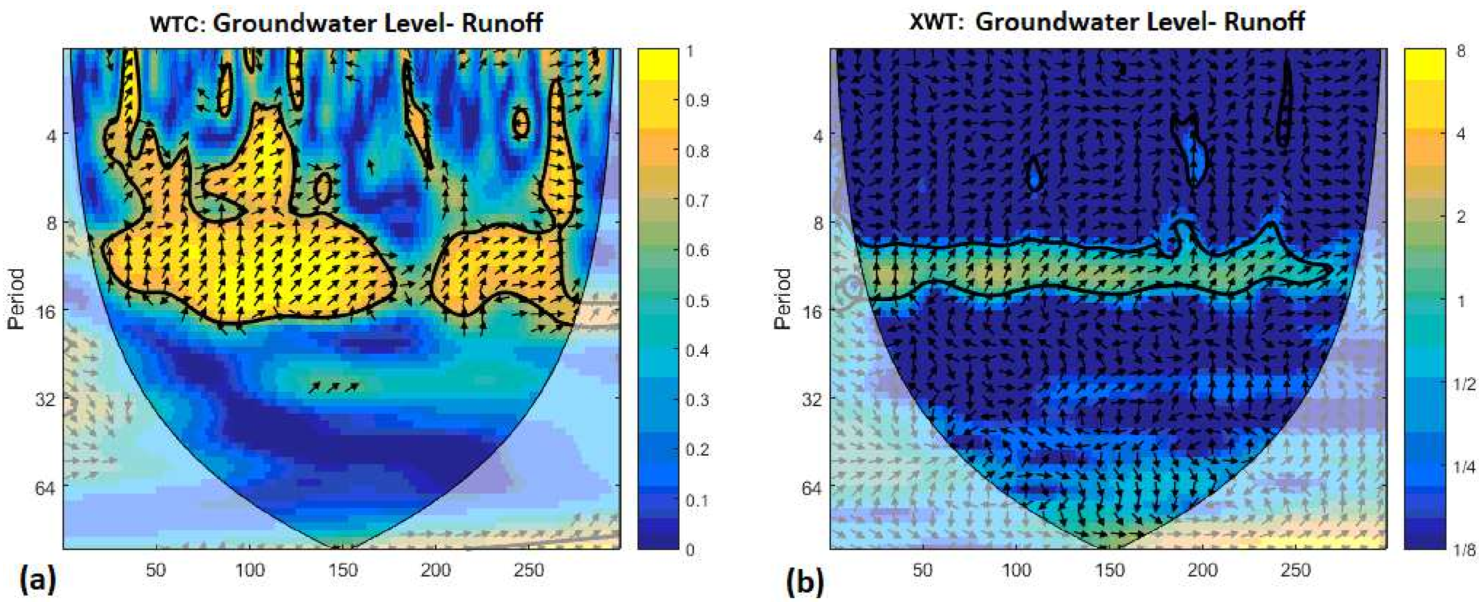

Figure 5

a) WTC and b) XWT between rainfall and GWL time series